

## 1 Title

2 Multiple energy carrier optimisation with intelligent agents

## 3 Authors

4 Spyros Skarvelis-Kazakos<sup>a,1</sup>, Panagiotis Papadopoulos<sup>b</sup>, Iñaki Grau Unda, Terry Gorman<sup>a</sup>, Abdelhafid Belaidi<sup>a</sup>, Stefan  
5 Zigan<sup>a</sup>

## 6 Affiliations

7 <sup>a</sup> Faculty of Engineering and Science, University of Greenwich, Chatham Maritime, ME4 4TB, UK

8 <sup>b</sup> Future Networks, UK Power Networks, London UK

## 9 Abstract

10 Multiple energy carrier systems stem from the need to evolve traditional electricity, gas and other energy systems to  
11 more efficient, integrated energy systems. An approach is presented, for controlling multiple energy carriers,  
12 including electricity (AC or DC), heat, natural gas and hydrogen, with the objective to minimise the overall cost  
13 and/or emissions, while adhering to technical and commercial constraints, such as network limits and market  
14 contracts. The technique of multi-agent systems (MAS) was used. The benefits of this approach are discussed and  
15 include a reduction of more than 50% in the balancing costs of a potential deviation. An implementation of this  
16 methodology is also presented. In order to validate the operation of the developed system, a number of experiments  
17 were performed using both software and hardware. The results validated the efficient operation of the developed  
18 system, proving its ability to optimise the operation of multiple energy carrier inputs within the context of an energy  
19 hub, using a hierarchical multi-agent system control structure.

20 **Keywords:** multiple energy carriers, energy hubs, distributed generation, microgrids, multi-agent systems

## 21 1 Introduction

22 It is expected that controllable loads and energy storage devices will be integrated in distribution networks of the  
23 future, in addition to distributed generation, thus increasing network complexity [1], [2]. Combined Heat and Power  
24 (CHP) generation technologies are also expected to form part of this generation mix [2], [3]. All these resources can be  
25 described as Distributed Energy Resources (DER).

26 CHP generators can utilise a number of different energy carriers as input fuels, such as natural gas or hydrogen.  
27 These carriers are delivered through different networks, which influence the overall efficiency and characteristics of a  
28 local energy system, including electricity networks. It has been proposed in [4], [5] and [6] that these energy carriers  
29 should be included in the design and planning phases of an energy system. In [6], an infrastructure planning tool was  
30 proposed for the design of energy systems in which heat and electricity carriers are coupled. Combined network  
31 analysis methodologies have also been developed [7]. In [8], a tool for integrating economic dispatch and optimal  
32 power flows of electricity and gas at the Grid Supply Points of Great Britain has been presented. Electric vehicles can  
33 also play a role as mobile resources in multiple energy carrier systems, and this has been discussed in [9] and [10].

34 It is necessary to evolve traditional electricity, gas and other energy systems to more flexible, integrated energy  
35 systems [11], referred to as multiple energy carrier, or multi-carrier systems. The points of interaction between  
36 different energy carriers have been described as “energy hubs” [5], [12], which present an integrated approach for  
37 optimizing systems with multiple energy carriers, such as electricity, hydrogen, or natural gas networks [13]. Devices  
38 are incorporated in an energy hub with the purpose of converting from one carrier to another, e.g. a CHP unit  
39 converting natural gas to electricity and heat. Storage elements such as batteries or thermal storage may also be  
40 considered. The energy carrier inputs to the energy hub are optimised and controlled in order to supply a given set of  
41 energy carrier loads / outputs, thus achieving whole-system optimization [12], [14]. In (1), the backward coupling  
42 matrix ( $D_{nm}$ ) which links the inputs ( $P_m$ ) with the outputs ( $L_n$ ) is shown, as this is a formality that is used in Section 2.2.  
43 The elements of the  $D_{nm}$  matrix are constructed using the conversion efficiencies of individual devices in the energy  
44 hub [12]. Matrix dimensions are  $M \times 1$ ,  $N \times 1$  and  $M \times N$ , for  $P_m$ ,  $L_n$  and  $D_{nm}$  respectively.

$$\begin{array}{c} \begin{bmatrix} P_\alpha \\ \vdots \\ P_\xi \end{bmatrix} = \begin{bmatrix} d_{\alpha\alpha} & \dots & d_{\alpha\xi} \\ \vdots & \ddots & \vdots \\ d_{\xi\alpha} & \dots & d_{\xi\xi} \end{bmatrix} \begin{bmatrix} L_\alpha \\ \vdots \\ L_\xi \end{bmatrix} \\ \underbrace{\hspace{1.5cm}}_{\text{input } P_m} \quad \underbrace{\hspace{1.5cm}}_{D_{nm}} \quad \underbrace{\hspace{1.5cm}}_{\text{output } L_n} \end{array} \quad (1)$$

48 A dispatch factor  $v$  is defined, which indicates the percentage of any given input that is being used by any given hub  
49 element in matrix  $D_{nm}$  [12]. For example, in (1), if  $d_{\alpha\alpha} = v_1 \times \eta_1$  and  $d_{\alpha\xi} = v_2 \times \eta_2$ , then  $v_1 + v_2 = 1$  where  $v_1$  and  
50  $v_2$  are dispatch factors of conversion devices in the energy hub and  $\eta_1$  and  $\eta_2$  their conversion efficiencies. Therefore,  
51 (1) can be used to calculate the total energy inputs ( $P_m$ ) required to satisfy a desired energy output [12]. Optimisation

<sup>1</sup> Corresponding author. Tel.: 0044 1273 877352. E-mail: sskazakos@theiet.org. Present address: Department of Engineering and Design, School of Engineering and Informatics, University of Sussex, Brighton, BN1 9QT, UK

1 methods are used to minimise the total energy inputs ( $P_m$ ) by varying the dispatch factors of the individual devices in  
2 the energy hub and consequently in the  $D_{nm}$  matrix. The problem is normally linear, but can become non-linear if  
3 generator part-load conversion efficiencies are taken into account, as their curves are non-linear.

4 Multi-agent systems (MAS) comprise multiple individual intelligent agents, e.g. installed on a controller of a DER.  
5 MAS are classified as a distributed control architecture and have been proposed as a promising technology for  
6 addressing control and co-ordination issues in the power industry, including DER [15], [16]. In addition, MAS have  
7 been proposed for controlling CHP unit clusters [17] and for co-ordinating electric vehicle charging [18],[19],[20],[21].

## 8 **1.1 Related work**

9 The concept presented in this paper combines the multiple energy carrier modelling approach of energy hubs, with  
10 the distributed control approach of multi-agent systems. The two concepts are inherently linked by the fact that they  
11 are both applicable mostly to distributed energy generation, i.e. local and small rather than central and large power  
12 plants. This link is thoroughly analysed in [22] and [23]. The comprehensive review of optimisation methods in multi-  
13 generation systems done in [22] reveals that a wide variety of centralised optimisation algorithms have been used.  
14 That includes traditional methods such as linear programming [24] and Lagrangian multipliers [25], as well as artificial  
15 intelligence (AI) algorithms such as evolutionary [26] and genetic algorithms [27]. Robust Optimization (RO)  
16 techniques have also been proposed in [28].

17 On the other hand, a wider conceptual view of the use of multi-agent systems in a market-like structure with  
18 multiple layers has been proposed in [29]. Agent-based implementations are by definition market oriented, provided  
19 that they use cooperative or competitive negotiation and coordination techniques, and normally use market-like  
20 structures to reach an optimal or near-optimal solution [29], [30]. Such market-oriented approaches have also been  
21 developed by the authors in previous work [18],[19],[20],[21]. The key design considerations for agent-based  
22 implementations most frequently encountered in the aforementioned literature are:

- 23 (a) The need for a commercial interface, which enables access to markets (e.g. power, ancillary services) [18], [19],  
24 [20], [21], [29], [31], [32], [33].
- 25 (b) The need for a technically-oriented supervisory structure, which is responsible for ensuring that the operation  
26 of the controlled/optimised resources adheres to technical limits of the infrastructure (e.g. voltage statutory  
27 limits, transformer ratings) [18], [19], [20], [21], [31].
- 28 (c) Agents typically possess cognitive abilities, such as complex communication and negotiation algorithms [15],  
29 [16], [29]. The responsive characteristics are very important in real-time power system operation, where time  
30 is often insufficient for high-level cognitive functions or communication (e.g. responding to faults).
- 31 (d) Hierarchical systems generally resemble the structure of power systems in terms of voltage levels, hence can  
32 be considered more suitable than their centralised or distributed counterparts [18], [19], [20], [21], [29], [31].
- 33 (e) The need to address or compensate for planning errors, including operation forecasts [21], [33], [34].

34 The combined use of multi-agent systems and energy hubs was implied in [9] and [35], where the focus was on  
35 electric vehicles, as well as [36], where an agent-based optimal power flow (OPF) solution was proposed for multiple  
36 energy carriers. The use of an agent-based algorithm for economic dispatch of power systems with wind penetration  
37 has been proposed in [37].

## 38 **1.2 Main contribution of the paper**

39 This paper extends the current state of the art, as shown in the literature review, by proposing an integrated  
40 technical and market-enabled approach to the control of multiple energy carrier systems, using an agent-based  
41 implementation. The main contribution of this paper is the validation of a novel control methodology for controlling  
42 multiple energy carriers with multi-agent systems. This methodology was initially described in [10] and its unique  
43 contribution is that it enables interaction of the energy hubs with external markets for procuring energy carriers. An  
44 additional contribution of this methodology is that it can cater for forecast inaccuracies, by facilitating an internal  
45 collaborative balancing mechanism, thus preventing deviations from procurement contracts that may lead to  
46 monetary penalties. An implementation of the methodology is presented, as well as case studies, which verify its  
47 validity. The case studies include simulations as well as experimental work.

## 48 **1.3 Structure of the paper**

49 The paper is arranged as follows. Section 2 describes the control approach; Section 3 presents the results of a  
50 simulated case study and Section 4 the results of an experimental study that validates the feasibility of the agents in  
51 real micro-CHP systems. Finally, the main conclusions and future work are discussed in Section 5.

# 52 **2 Multiple energy carrier optimization with intelligent agents**

## 53 **2.1 Agent-based control structure design**

54 The proposed control structure includes a number of agents, with different roles. Agents are linked to each of the  
55 elements in the energy hub. These agents hold detailed information on the state and characteristics of the device they

are linked to (e.g. a CHP generator agent has knowledge of CHP heat to power ratio, engine temperature, generator efficiency).

A hierarchical aggregation structure has been proposed, to enable the scalable and modular aggregation of the energy hubs [10]. A commercial aggregation entity is assumed as the highest level of aggregation. This entity operates as a Virtual Power Plant aggregator, interacting with wholesale electricity, gas, ancillary services or emissions markets, as described in [21]. A diagram illustrating the architecture of the system is presented in Fig. 1. The agent-based control structure includes four different agent types, with the following functions:

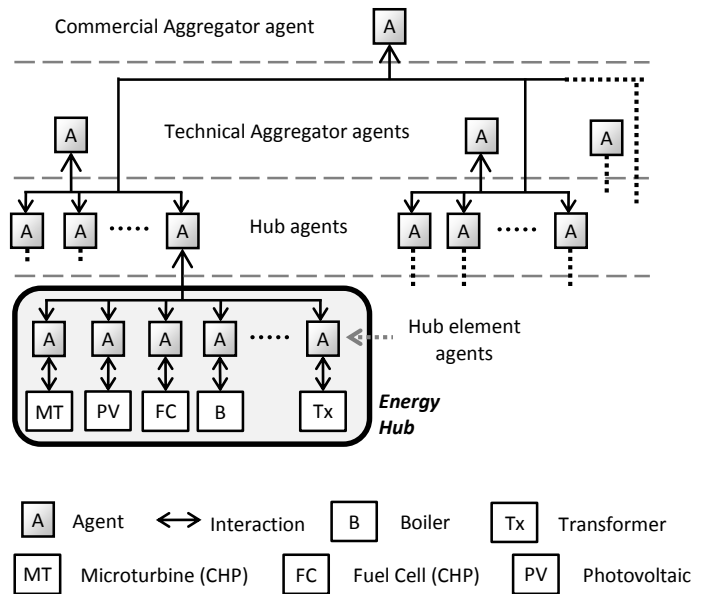


Fig. 1. Intelligent agent control architecture for energy hubs

The parameters include conversion efficiencies, heat to power ratio, availability and responsiveness. The parameters that a hub element agent has access to are given in Table 1. The Hub element agents are able to forecast stochastic parameters, such as wind speed, and adjust their limit, rating and efficiency values accordingly.

- **Hub element agents:** These represent micro-generators, electric vehicles, energy storage devices, boilers, controllable loads, converters, reformers. They can forecast demand and control generation, having visibility of the real-time parameters of their associated device for each of the relevant energy carriers. Such parameters include conversion efficiencies, heat to power ratio, availability and responsiveness. The parameters that a hub element agent has access to are given in Table 1. The Hub element agents are able to forecast stochastic parameters, such as wind speed, and adjust their limit, rating and efficiency values accordingly.
- **Hub agent:** Optimises the energy carrier inputs in the energy hub, according to the parameters provided by the hub elements and user preferences and needs. The Hub agent optimisation objectives are further discussed in the following section.
- **Technical Aggregator (TA – Microgrid) agent:** Validates that the optimised generation ( $P_m$ ) and demand ( $L_n$ ) forecasts from groups of Hub agents in the same local segment (e.g. electricity at the LV distribution transformer) are within technical constraints (e.g. power ratings, voltage levels, gas pressure). If they are not, a corrective action is requested, as described in Section 2.3 below.
- **Commercial Aggregator (CA – Virtual Power Plant) agent:** Trades energy carriers and services in appropriate markets. If there is a variation from market contracts, it requests from the Hub agents to adjust specific energy carriers associated with generation ( $P_m$ ) or demand ( $L_n$ ) (e.g. more electricity, less gas).

Table 1 – Parameters that Hub element agents were considered to have access to.

Hub element	Parameters
Photovoltaic	solar irradiation, cell temperature, module DC voltage / current, inverter AC voltage / current
Wind turbine	wind speed, rotor speed / torque, generator AC power output
Fuel Cell	cell temperature, fuel / oxygen / air flow rate, cell DC voltage / current, inverter AC output, CHP system input / output temperature, thermal power output
Microturbine	turbine rotational speed, fuel flow rate, shaft torque, generator power output, CHP system input / output temperature, thermal power output
Energy storage	battery State of Charge (SoC), State of Health (SoH), full-load and no-load voltage

## 2.2 Energy carrier optimisation in an Energy Hub

The Hub agent is responsible for optimizing the energy hub. Every time step that the optimisation is performed, the Hub agent collects data from all the hub element agents on conversion efficiency, input and output limits and resource forecasts for the next time step, where applicable. It then constructs the  $P_m$ ,  $L_n$  and  $D_{nm}$  matrices and hosts the optimisation calculations. The optimiser needs to ensure that the load is satisfied, subject to the constraints imposed by the CA contracts and the TA technical limitations. The optimization outputs are the dispatch factors in matrix  $D_{nm}$ . The optimal dispatch factors are then sent to the hub element agents. A flowchart describing the energy hub optimization algorithm is presented in Fig. 2. The optimisation is performed by varying the power inputs and/or the dispatch factors. The objective function  $F_{obj}$  of the optimisation problem is given in (2) below, where  $C_{obj}$  indicates a factor relating to the objective, as described in (a), (b) and (c) below:

$$\min F_{obj} = C_{obj} \sum_{m=1}^M P_m = C_{obj} \sum_{m=1}^M D_{nm} L_n \quad (2)$$

Three different objectives are considered in the optimization process:

- a) **Minimize total energy input:** Minimize total input energy consumption for the given loads, improving overall hub efficiency. In this case,  $C_{obj} = 1$  at all times.
- b) **Minimize total cost:** Modify the objective function, to include the cost of each energy carrier. Each row of the product of  $L_n D_{nm}$  is multiplied with a cost factor  $C_{obj}$  (e.g. £0.4 per  $m^3$  of natural gas).
- c) **Minimize total output emissions:** Similar to cost optimization, each row of the product of  $L_n D_{nm}$  is multiplied with an emission factor  $C_{obj}$  (e.g. 1.875  $kgCO_2/m^3$  of natural gas).

The formulation of the above optimisation problem in (2) is very similar to the agent-based objective of maximisation of social welfare, as described by (3), taken from [38], where  $sw(\omega)$  denotes the sum of utilities of each agent  $u_i$  of a set of agents  $Ag$ , for outcome  $\omega$ . In this case,  $\omega$  is equivalent to the Hub element agent's power input.

$$sw(\omega) = \sum_{i \in Ag} u_i(\omega) \quad (3)$$

Hence, by combining (2) and (3) and defining  $D_{nmi}$  as the coupling matrix of the individual Hub element agents, the maximisation of the agent social welfare consists of minimising the objective function:

$$max[sw(\omega)] = min \left[ C_{obj} \sum_{m=1}^M \left( \sum_{i \in Ag} D_{nmi} \right) L_n \right] \quad (4)$$

Optimisation constraints include operational constraints (power ratings) of energy hub devices, energy storage capacity and external infrastructure constraints at the power input ports [10], [14]. The following constraints are common constraints which may be encountered in a realistic system:

- **Carrier supply limitations**, where  $P_{min}$  and  $P_{max}$  is the minimum / maximum power input that the infrastructure can support. This can be due to e.g. transformer ratings for electricity, or gas network minimum pressure limits. The lower limit may be zero or negative, depending on the approach to reverse power flow, i.e. whether the reverse power flow can be considered as a negative input or as an output. The calculation of this constraint can also come from a power flow analysis of the external electricity network, as in [14].

$$P_{min} \leq P_m \leq P_{max} \quad (5)$$

- **Hub element equipment limitations**, such as minimum / maximum generation output  $Gmin_n$  and  $Gmax_n$ , for carrier  $n$  and element  $i$ . This is typically defined by power output ratings of the conversion equipment for each carrier. In the case of energy storage,  $Gmin_n$  could extend to negative values.

$$Gmin_n \leq L_n^i \leq Gmax_n \quad (6)$$

- **Dispatch factor complementarity**, for the same energy carrier  $n$ , since the amount of energy carrier input that is fed to each element  $i$  is defined proportionally to the dispatch factors.

$$v_1^n + v_2^n + \dots + v_i^n = 1 \quad (7)$$

- **Closed system constraint**, which dictates that the inputs matrix  $P_m$  must equal the outputs matrix  $L_n$  multiplied with the coupling matrix  $D_{nm}$ . This is effectively the same as equation (1).

$$P_m = D_{nm} L_n \quad (8)$$

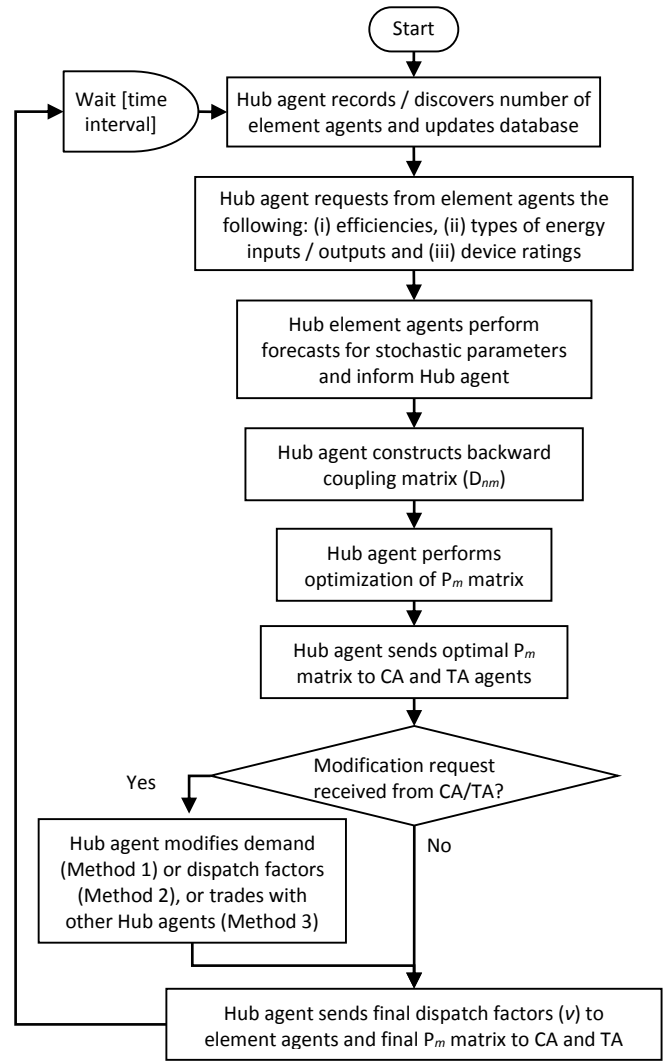


Fig. 2. Energy hub optimization algorithm

### 2.3 Agent-based multiple energy hub interaction

The optimization algorithm is processed for as long as the system remains operational, at pre-defined time intervals (in this paper half-hour intervals are used, in accordance with market contracts in the UK wholesale market). At each time interval, the objective function for the next time interval is optimized, as seen in [8], [10] and [31]. A major concern is the potential for forecast errors, which carries the risk of mismatch between calculated optimal dispatch of energy hub elements and available energy carrier inputs procured by the Commercial Aggregator agent. This is what the proposed multi-agent system intends to solve, by facilitating a collaborative balancing mechanism. A Unified Modelling Language (UML) diagram of the interaction between the different agents is shown in Fig. 3. Once the optimal energy hub inputs are calculated for a time-step/interval, then the Hub agent informs the Commercial and Technical Aggregator agents of its calculated  $P_m$  matrix. If a mismatch is found due to energy availability or if technical constraint violations are foreseen, the CA or TA agents respectively calculate the difference (shortfall or excess) and inform the affected Hub agents. The Hub agents then take one or more of the following actions. The decision on the choice of method is based on the nature of the mismatch. This is further discussed in Section 3.4.

- Method 1:** Modify demand ( $L_n$ ) characteristics of the energy hubs by means of controllable loads.
- Method 2:** Modify the dispatch factors of the hub elements away from the optimal position, changing the input characteristics ( $P_m$ ).
- Method 3:** Trade energy carriers between them (e.g. 1 kWh electricity, 1m<sup>3</sup> natural gas), if possible, to maintain the hub optimal positions.
- Reject a CA modification request, initiating a compensation process, where the CA either negotiates an alternative contract, or receives a penalty from the market. Requests from the TA cannot be rejected, due to technical constraints.

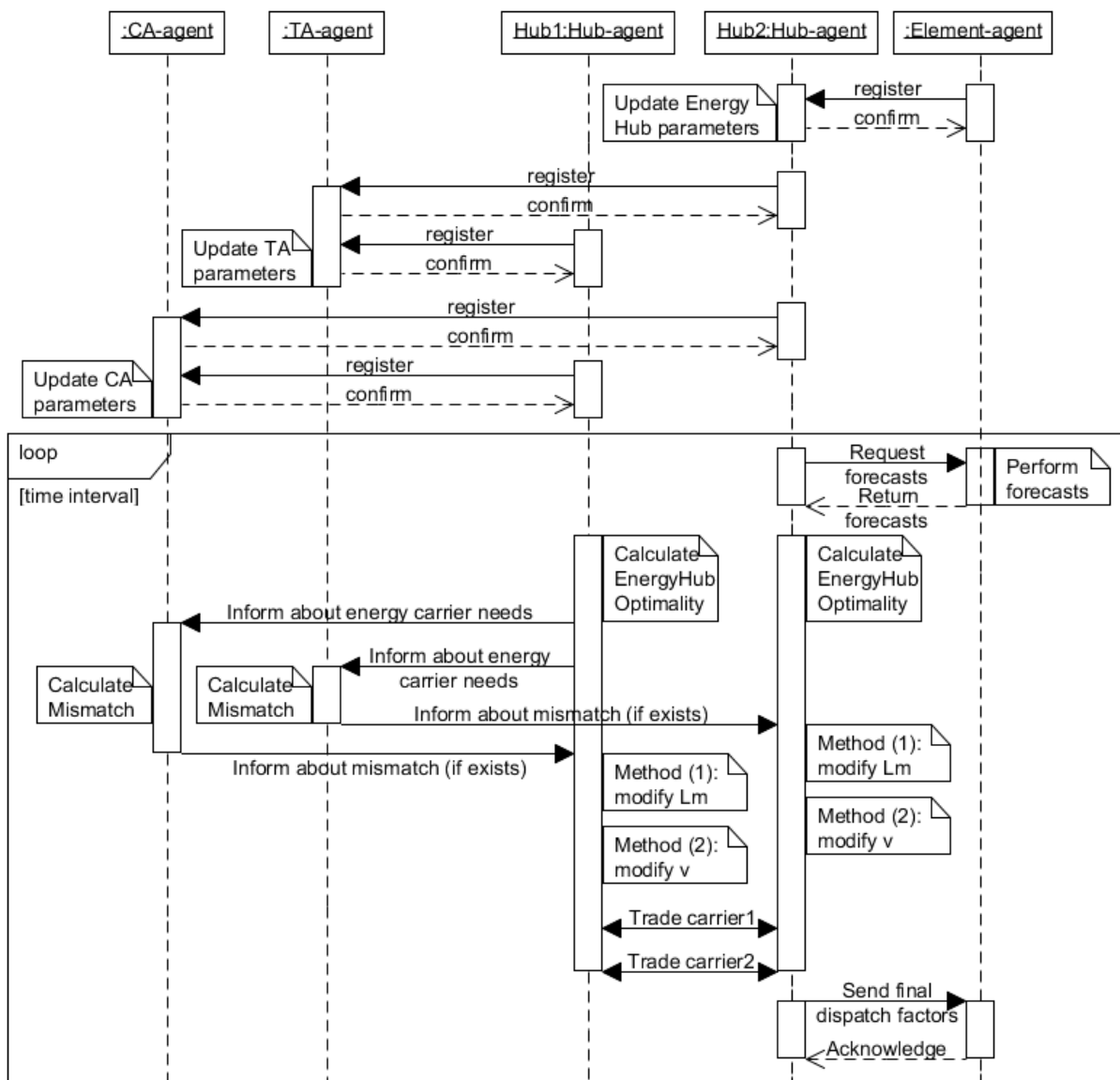


Fig. 3. UML diagram of the multi-agent system interactions

## 2.4 Co-ordination mechanism

The mechanism for co-ordinating multiple energy hubs in Method 3 is a first-price sealed-bid auction [38]. This is the simplest form of auction, involving just one round of bidding. The Hub agent that wants to trade energy carriers (initiator) sends out a call for proposals. Then, any other Hub agent which is interested in trading (responder) submits a bid and the initiator agent allocates the traded energy carrier to the highest bidder. Fig. 4 shows the UML diagram of this interaction.

## 2.5 Comparison with other methodologies

The proposed methodology is aimed at improving certain weaknesses of traditional centralised optimisation methodologies, hence indicators such as optimality or computational time or efficiency are not appropriate to use in the comparison. However, an attempt is made in Table 2 to compare these indicators, as well as the functionality of the proposed methodology against centralised linear optimisation. The functionality benefits by the proposed methodology match those of multi-agent systems in general, as these have been described in [16].

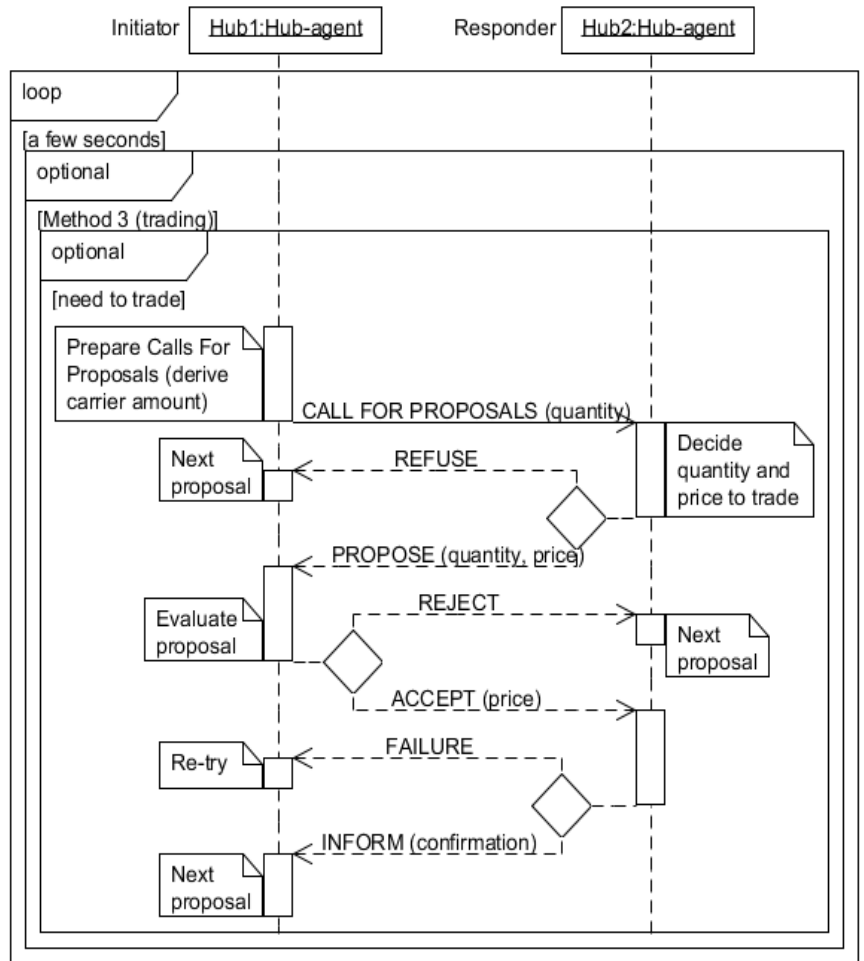


Fig. 4. UML diagram of the Hub agent bidding mechanism

Table 2 – Functionality of proposed methodology against traditional centralised optimisation.

Functionality indicator	Proposed methodology	Centralised linear optimisation
Computational time	Uncertain – depends on agent interaction, affected by communication delays, not limited by system size	Fast – but limited by size of system
Optimality	Near-optimal	Optimal
Scalability	Unlimited	Limited by computational capacity
Visibility	Complete, down to the equipment level	Limited to high-level parameters
Forecast error tolerance	Can compensate through Methods 1 / 2 / 3	None – optimisation algorithm must be repeated

## 3 Simulated case study

### 3.1 Motivation

The nature of the proposed methodology involves a large number of energy resources, such as distributed generators, energy storage devices and electric vehicles. Multi-agent systems such as the proposed system are scalable [16], so could range from a handful to thousands of resources. Hence, it is not practical to attempt a full-scale experimental verification, since that would require a large-scale field trial to be meaningful. Instead, a simulated case study was built, in order to test the functionality of the control system implementation.

### 3.2 System description and input data

The studied system is a microgrid, based on the system described in [3]. The microgrid includes a total electrical generation capacity of 63kW, comprised of the distributed generation (DG) units in Table 3, as well as 20 households. Two optimisation targets were considered in separate case studies: (i) cost reduction and (ii) CO<sub>2</sub> emissions reduction. The carrier inputs considered are (i) renewable energy in the form of wind or solar energy, (ii) grid electricity and (iii) natural gas. The output carriers considered were (i) electricity and (ii) heat. A large boiler was considered as a backup

1 heat source and the electricity grid as a backup  
 2 electricity source. The boiler and CHP units were fed  
 3 by natural gas and the electricity output was linked to  
 4 the input through a transformer. Fig. 5 shows the  
 5 energy hub structure considered. Two identical energy  
 6 hubs were included in the model.

7 The cost was taken as £0.1558 per kWh for grid  
 8 electricity and £0.05013 per kWh for natural gas [39].  
 9 Emission factors were taken as 430 gCO<sub>2</sub>/kWh for grid  
 10 electricity and 184 gCO<sub>2</sub>/kWh for natural gas [40].  
 11 Daily half-hour electrical load profiles from [41] were  
 12 used and thermal load profiles from [42]. The  
 13 electrical load profiles were scaled to the maximum  
 14 electrical load of 116.4 kVA at a power factor of 0.85,  
 15 as in [3]. The thermal load profiles were scaled to 8  
 16 kW per household [42], for 22 units (20 households  
 17 and 2 service areas) [3]. Natural gas is supplied to the  
 18 fuel cell, the microturbine and the boiler. Electricity is  
 19 fed to a transformer, while renewable energy (wind  
 20 and solar) is input to the wind turbine and  
 21 photovoltaic. JADE (Java Agent Development  
 22 Framework) was used to model the MAS. Optimisation of the energy hub was performed for each of 48 half-hour  
 23 steps using the open-source JOM (Java Optimization Modeler) package [43].

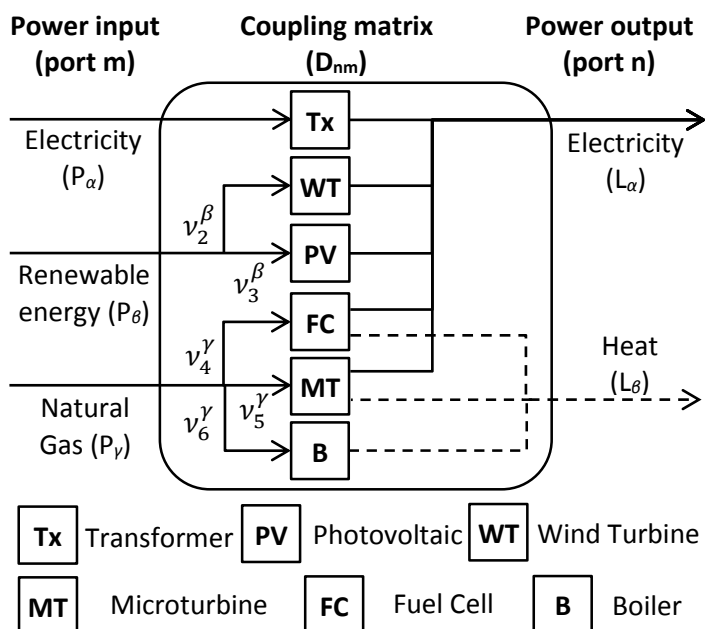


Fig. 5. The simulated energy hub, which includes three inputs in port m and two outputs in port n.

Table 3 – Energy Hub elements, their efficiency and power characteristics [3], [40].

Hub element	Electrical efficiency (%)	Thermal efficiency (%)	Electrical output (kW)	Thermal output (kW)
Photovoltaic	15	-	10	-
Wind turbine	40	-	13	-
Fuel Cell	40.4	56.6	10	14
Microturbine	25.9	67.34	30	78
Large boiler	-	90	-	3072
Grid transformer	98	-	500	-

### 3.3 Simulation results – impact of optimisation

Simulations were performed, testing the optimization of the system against (a) minimized cost and (b) minimized emissions. Additional simulations were performed to record the cost and emissions when the test system was not controlled / optimized, as a base case. It was assumed that the photovoltaic, wind turbine and fuel cell would constantly run at 100% of their output capacity. The microturbine would also run at full capacity, unless the load was not enough to absorb the output power (no ability to feed power to the grid). The grid and the boiler would supply any additional electrical or thermal load respectively. The load was considered the same in all cases (see Section 3.2). This base-case scenario is consistent with the fit-and-forget approach currently in place in the generation industry.

Fig. 6 illustrates the impact that the optimisation has had on the cost (in £/kWh) and emissions (in gCO<sub>2</sub>/kWh) of one of the energy hubs, by comparing the optimised with the non-optimised results. The average reduction throughout the day was found to be **6.42%** in cost and **14.10%** in emissions.

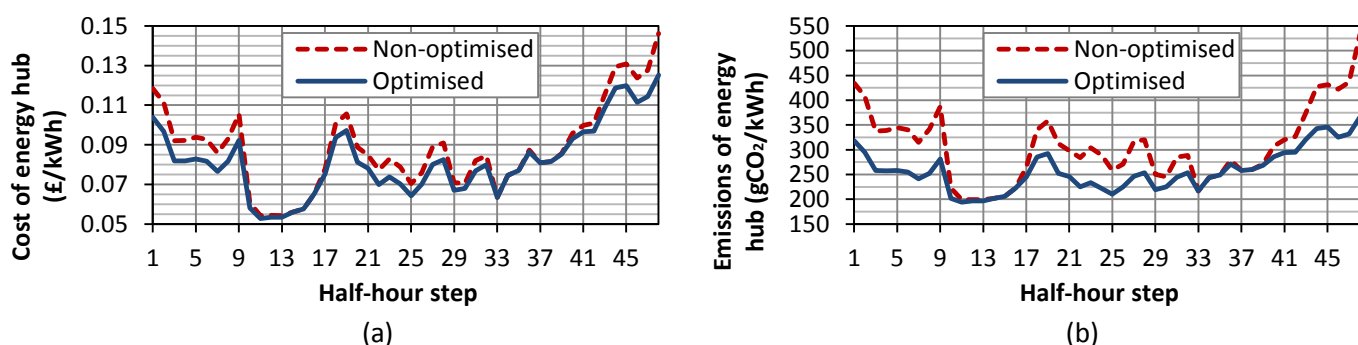


Fig. 6. Optimised against non-optimised cost (a) and emissions (b) per kWh of energy hub inputs every half-hour

As can be seen from Fig. 7 below, the optimized profile of power inputs in one energy hub shows much reduced (21.8% on average) primary power consumption for feeding the same load, when compared to the non-optimized input profile. The graphs are cumulative, thus showing the total primary power input to the energy hub. An important factor is that the non-optimized operation of CHP generator(s) leads to heat being dissipated, which would otherwise be useful for feeding the thermal loads.

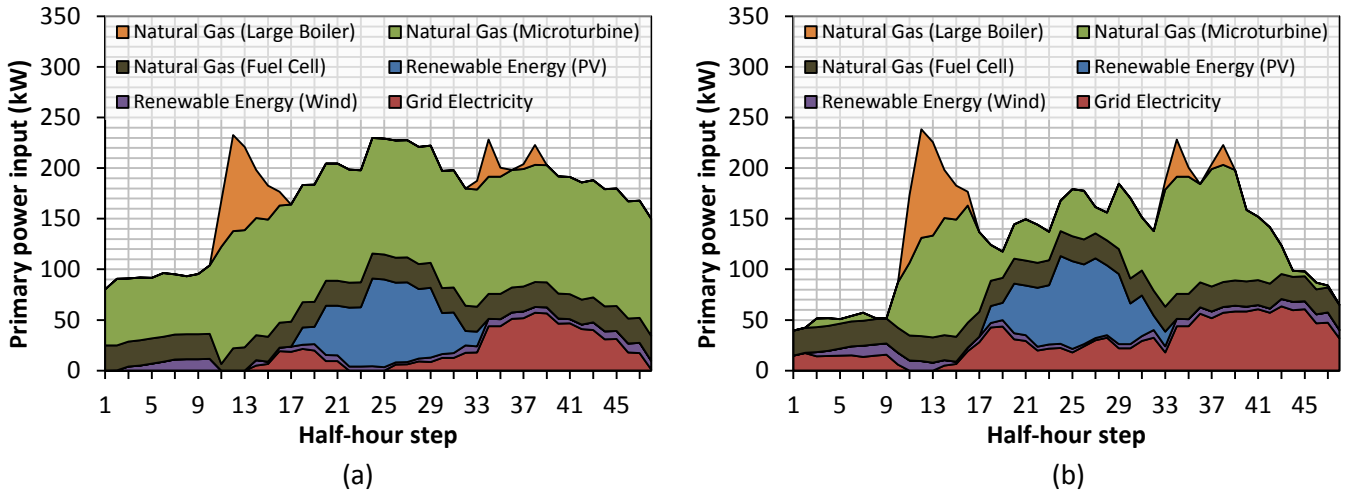


Fig. 7. Breakdown of (a) non-optimized and (b) cost-optimized energy hub primary power inputs every half-hour

### 3.4 Simulation results – effectiveness of balancing methods

A sensitivity analysis was performed to evaluate the effectiveness of the balancing methods. Deviation requests were initiated by the Commercial Aggregator agent, based on typical forecasting errors. An average load forecasting error of 3.45% is reported in [44]. For the studied system, this equates to **3.42 kW** for electricity and **6.08 kW** for gas. Hour-ahead forecast errors of up to 12.851% have also been reported in [45], which would translate to **12.71 kW** for electricity and **22.62 kW** for gas. Simulations were performed assuming a deviation request on each of the time-steps (every half-hour), to evaluate the times of the day when the proposed system would be more effective. The parameters that were varied in the sensitivity analysis are as follows:

- Magnitude of deviation, i.e. 3.42 kW or 12.71 kW for electricity and 6.08 kW or 22.62 kW for gas
- Direction of deviation, i.e. negative or positive (e.g. – 3.42 kW, + 22.62 kW) and all combinations
- If one or two energy hubs were affected.

It was assumed that if all three methods failed to take care of the deviation request, then the Commercial Aggregator would have to resort to the external balancing markets. Balancing costs were estimated at 0.003 £/kWh [46]. Fig. 8 presents a comparison between using the proposed system to internally balance deviations and going straight to the balancing market. Table 4 presents the average cost per kWh of the cases presented in Fig. 8.

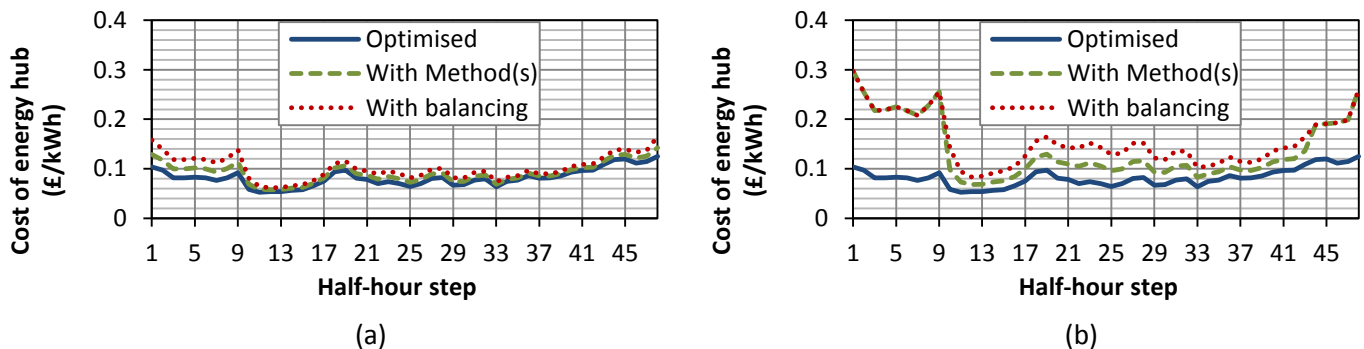


Fig. 8. Cost comparison between using the proposed system and resorting to external balancing markets for deviations of (a) +3.42 kW electricity and +6.08 kW gas and (b) +12.71 kW electricity and +22.62 kW gas

Table 4 – Comparison of average kWh cost between the proposed Methods and the external balancing market. The +12.71 kW<sub>electricity</sub> / +22.62 kW<sub>gas</sub> case only accounts for time-steps 10 – 43, where the Methods were used

	+3.42 kW <sub>electricity</sub> / +6.08 kW <sub>gas</sub>	+12.71 kW <sub>electricity</sub> / +22.62 kW <sub>gas</sub>
<b>Optimized – no deviation</b>	£0.0820 / kWh	£0.0755 / kWh
<b>Deviation resolved with Methods</b>	£0.0916 / kWh (+11.6%)	£0.1005 / kWh (+33.9%)
<b>Deviation resolved with external balancing market</b>	£0.1020 / kWh (+24.3%)	£0.1272 / kWh (+70.0%)

In Fig. 9, a breakdown of the primary inputs is given, per hub element, for one of the energy hubs that was simulated. Fig. 9(a) shows the normal optimised profile of an energy hub, without any deviation requests, with the characteristics described in Section 3.2. Fig. 9(b) shows the same profile, when a large deviation request of +12.71 kW for electricity and +22.62 kW for gas is received at every time step and resolved by Method 2. It can be seen that the total power input is much higher and the dispatch of energy hub elements is different, as it is now constrained by the requested deviation.

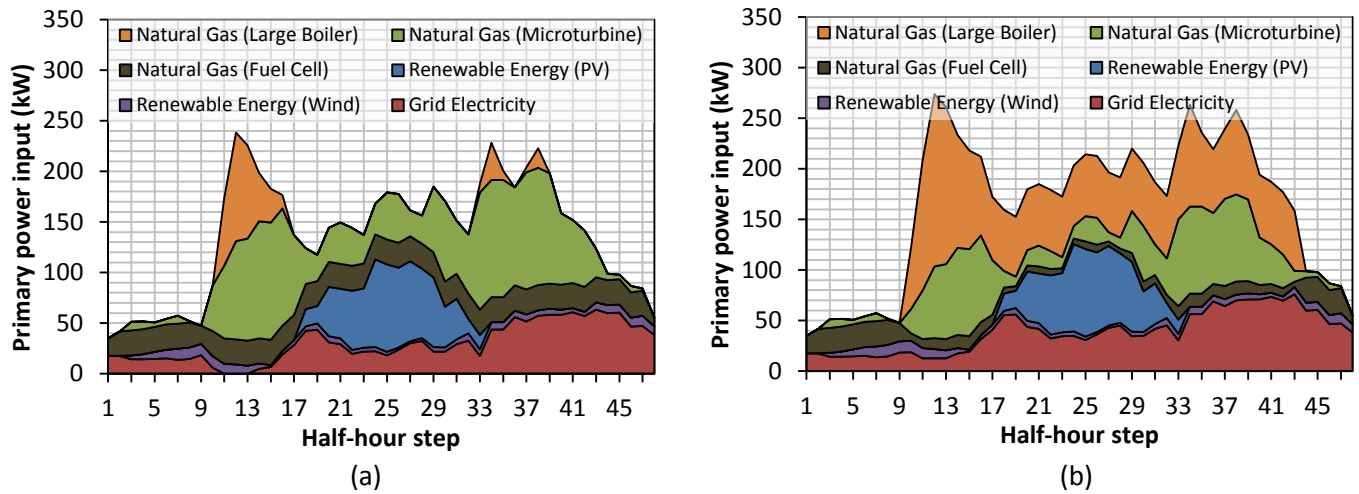


Fig. 9. Breakdown of the primary power input, for minimisation of energy hub inputs (a) without any modification requests (b) with large [+12.71 kW electricity / +22.62 kW gas] modification requests addressed by Method 2

### 3.5 Discussion of simulated results

The results shown in Fig. 6 and 7 prove that the developed system is able to optimise the operation of multiple generation units (CHP and renewable) with multiple energy carrier inputs within an energy hub, compared to a base case of non-optimised dispatch. Fig. 8 and Table 4 further show that the proposed system is more cost-effective in accommodating forecast errors than the existing balancing markets. In addition to the results presented in Sections 3.3 and 3.4, findings from the sensitivity analysis that was performed include the following:

- Method 1 was not able to resolve requests involving positive deviations. However, when negative deviations occurred, the average overall deviation was reduced by up to **81.9%**, leaving the remainder to be addressed by Method 2 or 3.
- In the case of deviation of +12.71 kW for electricity and +22.62 kW for gas for both Hubs, Method 2 was the only method which could resolve the deviation, but only in the peak periods. If such a deviation occurred during off-peak periods, the option to enter the external balancing market had to be chosen. This is apparent in Fig. 8(b), where the cost in the off-peak periods matches that of the external balancing market. This is most likely because during off-peak periods there would not be enough load to accommodate the additional requested consumption.
- In the case of deviation of +12.71 kW for electricity and +22.62 kW for gas for only one of the two Hubs, Method 3 resolved the deviation, but again only in the peak periods. Hub 1 was assumed to not be able to accommodate the deviation request, hence it traded with Hub 2. However, during off-peak periods Hub 2 was also unable to accommodate any deviation, for the same reasons described in point (b) above.

From the tests performed, it was observed that the distribution of the primary power input across the different energy hub elements is almost identical in both the cost and the emissions optimisation. The use of renewables is maximised in both cases, since the cost as well as emissions during their operation is assumed to be zero, given that life-cycle costs and emissions are not taken into account. Due to the power generation limitations of the local generators (CHP and renewables), grid electricity is used as a complementary resource, to fill in the gaps in electricity supply. Likewise, the backup boiler is operated only when the thermal load exceeds the capacity of the CHP units.

There is a requirement to supply a fixed load, and the optimised profile has been fine-tuned to do that with the minimum primary power input. Hence, there is very little room to reduce the power input of any of the carriers. This was apparent during the simulations, since the optimiser could not converge even with relatively small power input reduction requests from the aggregator. Conversely, due to the presence of the grid backup supply and the large boiler, the margin to adhere to power input increase requests was quite large. Thus, it can be concluded that Method 1 (using controllable loads to reduce load) must be used for reduction requests and Method 2 (modifying optimal

position) for increase requests. It was also seen that energy hubs can trade power inputs within their operating range using Method 3, being able to cover for each other's mismatch. However, a Hub agent receiving a request to cover a mismatch on behalf of another agent also needs to use Methods 1 or 2, to be able to comply.

The results in Table 4 also show that if the proposed system was used for dealing with forecast errors, the costs associated with balancing would be reduced by approximately **52%**, independent of the magnitude of the forecast error. However, the overall cost of energy would be reduced by approximately **10%** for the case of +3.42 kW electricity / +6.08 kW gas and **21%** for the case of +12.71 kW electricity / +22.62 kW gas, compared to the overall energy cost when using the external balancing market. Hence, the savings that can be achieved by the proposed system are directly proportional to the occurring forecast error.

A special case that may occur during the operation of the system is that the energy hubs may have conflicting objectives. If the aggregator requests all hubs to reduce e.g. their gas consumption, it is highly likely that some hubs will not be able to accommodate that request. Method 3 will be executed and through the internal trading mechanism the system will find the most appropriate way of sharing the requested reduction, with the least amount of overall mismatch. Hence, the energy that must be traded in the external balancing market is also minimised. This is realistically the best way of resolving such a scenario and is consistent with previous work by the authors and other researchers in the field of agent-based trading mechanisms [10], [15], [16], [17], [21], [29], [30], [32], [38].

#### 4 Technical feasibility of agent-based controllers in real domestic micro-CHP applications

##### 4.1 Motivation

The operation of the algorithm and multi-agent system was thoroughly tested in the previous sections. Distributed and agent-based systems do not rely on high-powered centralised data processing centres, but are aimed at utilising small-scale, low-powered, distributed computing and control hardware installed on local resources, much like the Internet of Things (IoT) paradigm. Hence, it is important to test if the developed system can be hosted in such hardware, especially since it involves optimisation, which can be computationally demanding. A schematic showing a breakdown of a typical installation of intelligent control equipment on DER is shown on the left side of Fig. 10. The communications systems feasibility has been proven by the authors in previous work involving an earlier version of the system, which had a much more intense communications burden [21]. It was shown that the agents can communicate effectively even through a dial-up internet connection. In this context, it was important to test further the interface of the agent platform with real multiple energy carrier conversion equipment (micro-CHP).

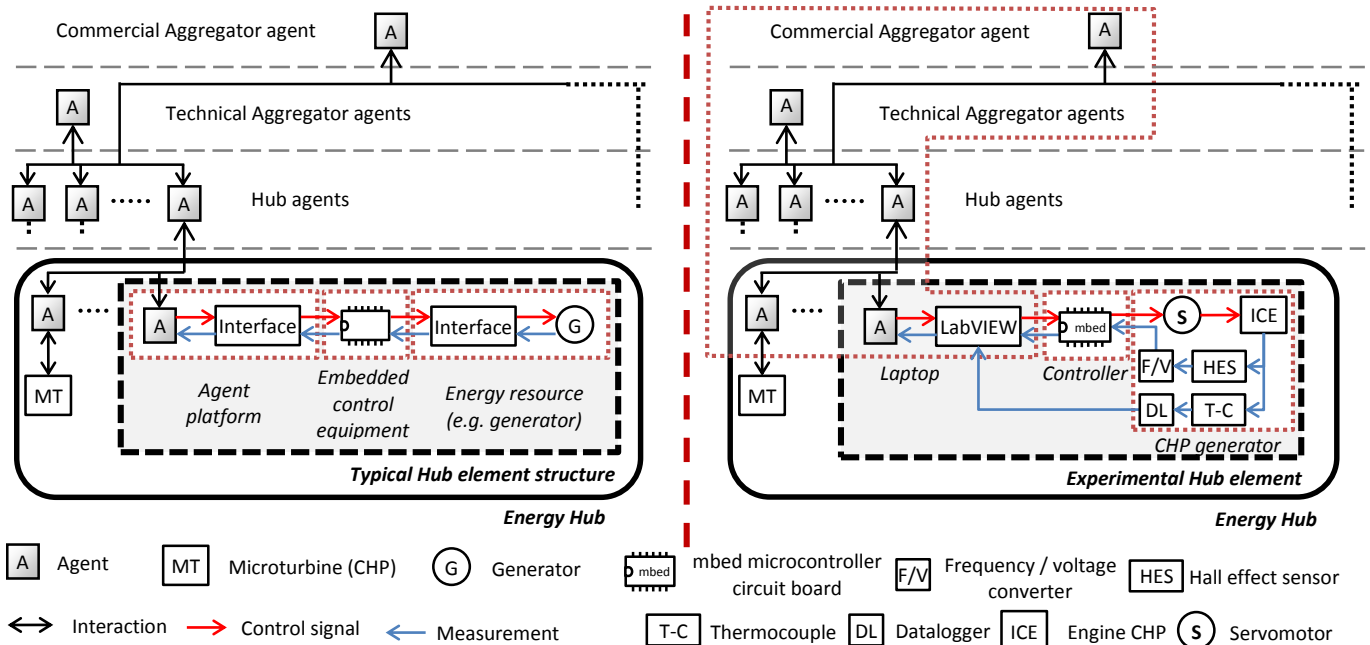


Fig. 10. Internal hardware structure of a typical Hub element (left) and the experimental setup (right), in the context of the multi-agent system

##### 4.2 Experimental setup description for testing the interface with micro-CHP equipment

The feasibility of the interface was tested using a micro-CHP unit test rig, shown in Fig. 11. The engine is a water cooled 4-stroke 2 cylinder Honda engine which produces 5.595 kW (7.5 hp), a size appropriate for domestic installations [3]. The engine is controlled by using a custom-made digital controller circuit-board interfaced with LabVIEW. The micro-CHP test rig was also retrofitted to include heat exchangers at the exhaust. The working fluid

used was tap water, extracting heat from the engine's exhaust gases. A trial run was undertaken to estimate the efficiency of the micro-CHP system. Both the electrical and thermal efficiencies were found to be 10%. Hence, thermal output was considered to be equal to the electrical output, 5.595 kW<sub>th</sub>.

The tests included linking LabVIEW to the JADE code and control the engine according to the multi-agent system decision-making process. The JADE code was receiving information from the instruments on the test rig and was feeding the decision-making set-points to the engine. This enabled the test of the control system with real feedback. A schematic of the system is shown on the right side of Fig. 10.

A servomotor was used to control the throttle, the setpoint for which was given by the agent through LabVIEW. LabVIEW was also logging data such as engine speed and water temperature at the input and output of the exhaust heat exchanger and was passing those measurements to the CHP agent. Due to the lack of an electric motor, the engine was assumed to run in constant torque mode. Since the power of rotating machinery is given as the product of torque and angular speed ( $P = \tau \times \omega$ ), the electrical output was taken to be proportional to the speed. The speed of the engine was determined by a Hall effect sensor and magnet arrangement on the shaft of the engine. The circuit-board had a frequency to voltage converter on board that took the pulses from the Hall effect sensor (on the shaft of the engine) and converted them to a voltage to be applied to the analogue input of the mbed microcontroller (see Fig. 10). The system was calibrated using a hand held optical tachometer. The speed of the engine was therefore proportional to the voltage applied to the analogue input of the mbed microcontroller.

The experiments were performed using a mid-range consumer laptop (Intel i3) to run the MAS code and the LabVIEW interface, also functioning as a data-logger. Two energy hub agents were simulated, with each energy hub containing 6 energy resource agents. Including the test rig agent, 15 agents were simulated in total. The optimisation process was performed twice in every time-step, once for each of the two energy hubs. The time-step was considered to be a half-hour, but due to engine run time limitations, each half-hour was considered to last 30 seconds. Two tests were undertaken:

- **Test 1:** A test with the measured efficiency (electrical = 10%, thermal = 10%). However, due to the very low efficiency of the engine rig, it was not being utilised by the optimiser and was constantly ran at the minimum. Hence, test (b) was also performed.
- **Test 2:** A test considering the engine to have the efficiency of a typical microturbine, as defined in [40] (electrical = 25.9%, thermal = 67.34%).

### 4.3 Experimental test results

The results from the experimental study are presented in Fig. 12 – 14. In Fig. 12, a breakdown is given of primary power inputs to the energy hub that the test rig was considered to be part of. The diagrams are cumulative and the engine petrol input (in kW) is at the bottom. Fig. 12(a) shows the results from Test 1 and Fig. 12(b) the results from Test 2. It is observed that the engine input in Fig. 12(a) is constant, which is explained in the discussion section.

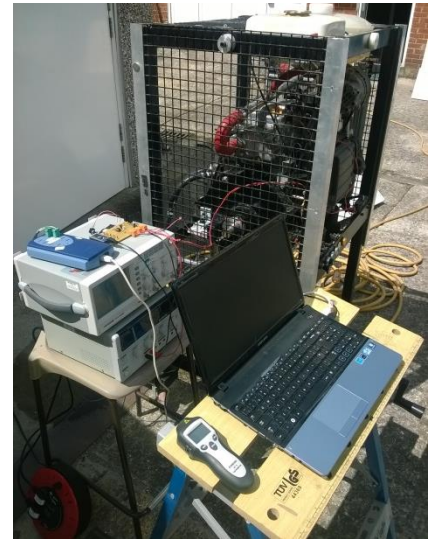


Fig. 11. The engine rig used in the tests

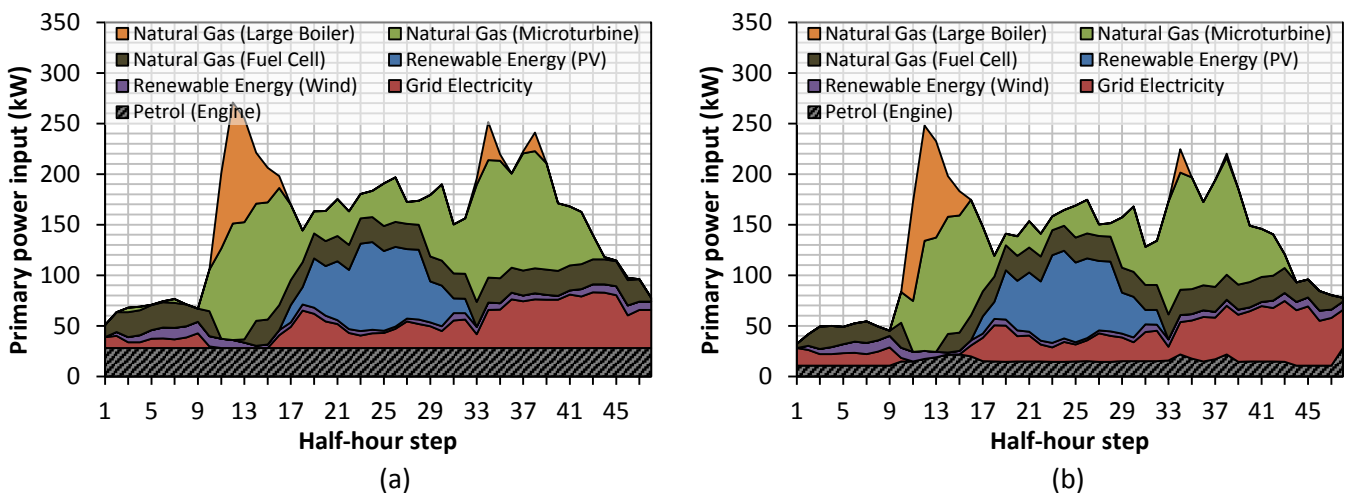


Fig. 12. Breakdown of the primary power input by resource for (a) Test 1 and (b) Test 2

The agreement of the fuel input setpoint given by the controller, with the actual fuel input recorded, is compared in Fig. 13. It can be seen that the deviation is small in Test 1, but larger in Test 2. This is because the fuel input was calculated using the electrical and thermal output measurements from the engine rig. Since in Test 2 the ratio of electrical and thermal output was different than the actual, an offset is observed. This can also be seen in Fig. 14.

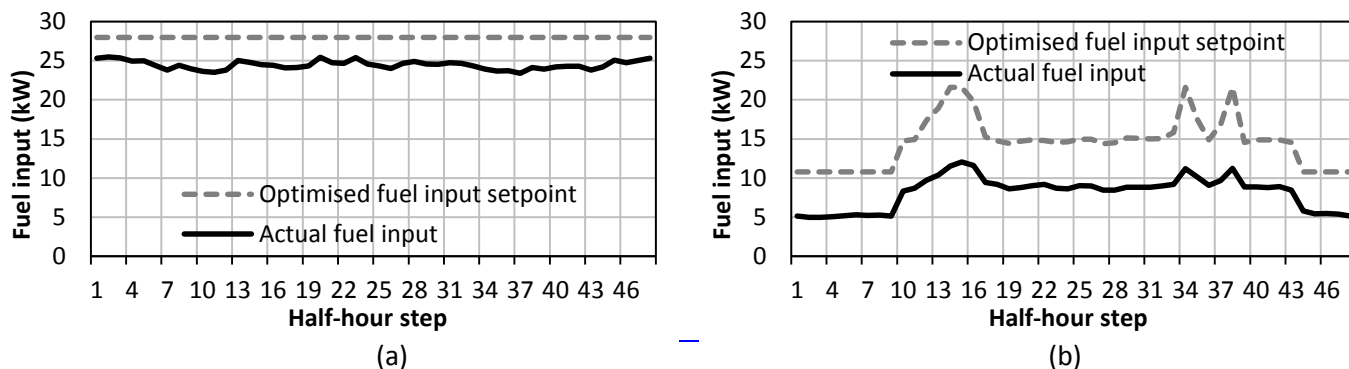


Fig. 13. Optimised (setpoint) and actual fuel input to the engine for Test 1 (a) and Test 2 (b)

In Fig. 14, the temperature range of the heat exchanger, as well as the calculated electrical and thermal output of the engine rig are shown for Test 1 in Fig. 14(a) and Test 2 in Fig. 14(b). It can be seen that during Test 1, the outputs are constant, at the minimum. This is due to the efficiency being comparatively very low, hence the multi-agent system operated the engine as low as possible to prevent the overall energy hub efficiency from dropping. This was the main reason that Test 2 was performed. During Test 2, the engine rig is utilised more, which is reflected in Fig. 14(b). The observed deviation between the setpoint and the actual engine thermal output in Test 2 is due to the difference between the real and the assumed ratio of electrical and thermal efficiencies. Since the engine was operated as electrically-led, this deviation in the heat output was unavoidable.

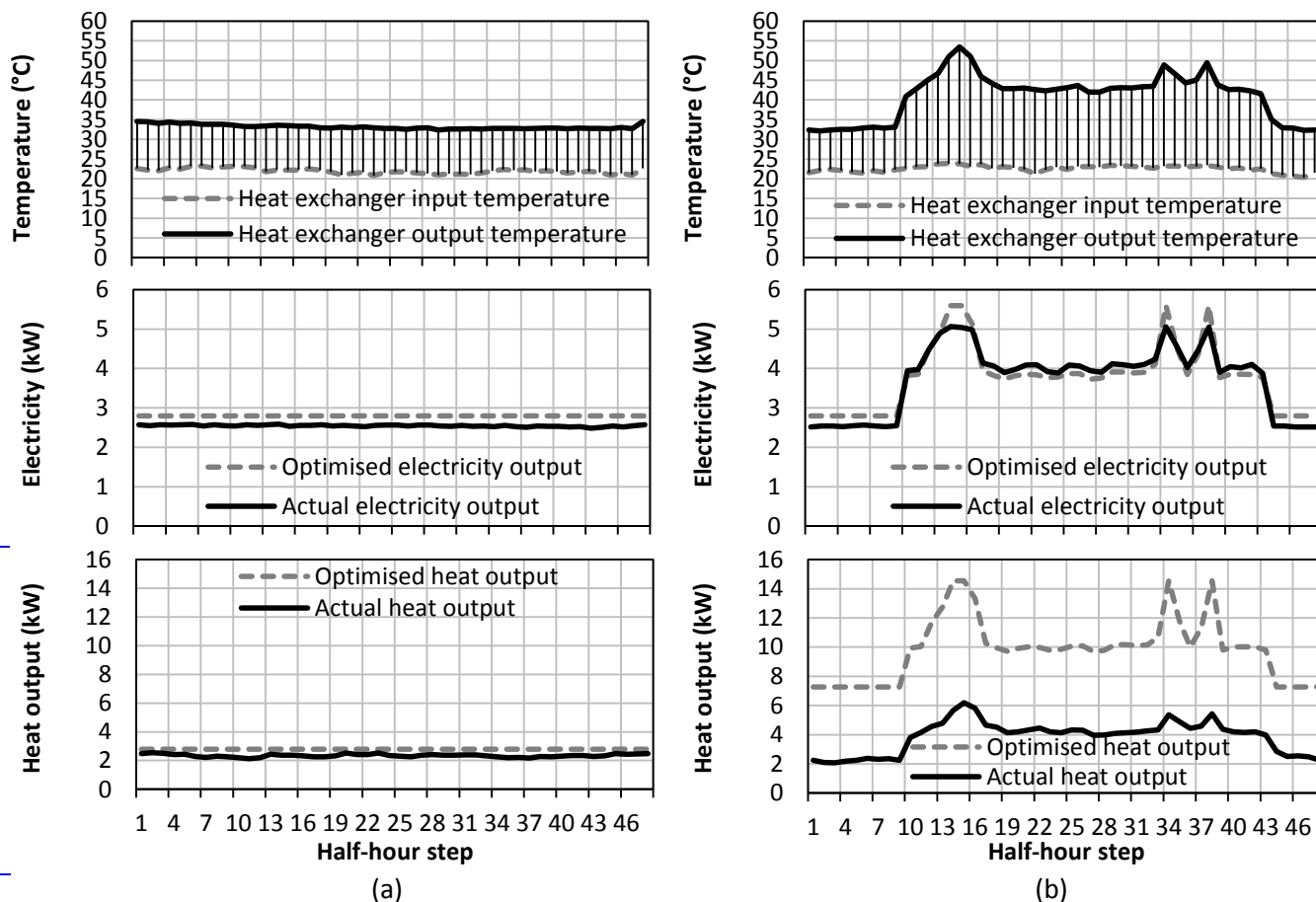


Fig. 14. Water input and output temperature to the heat exchanger, as well as optimised and actual electricity and heat output of the engine for (a) Test 1 and (b) Test 2

#### 4.4 Discussion of experimental results

The results of the experimental study show that it is feasible to control real energy resources with the proposed MAS. The test rig controller and agent-hosting platform (laptop) would be replaced by a commercial purpose-built device, able to host the agent, communicate with the other agents and control the energy resource. From Fig. 12, Fig. 13 and Fig. 14, it can be seen that the rig was utilised more when the efficiency was considered to be of a typical microturbine CHP, also reducing the overall primary power input, due to the reduced associated losses.

The whole computational time on the computer was measured in the range of **2.06 – 2.68 seconds**, to execute all Methods for the whole system (two energy hubs). Taking into account that time intervals were considered to be 30 minutes apart, the tested methodology is not very computationally intensive. Hence, inexpensive platforms with lower computational power (e.g. micro-controllers, single-board computers) may be used to host the agents. The controller platforms must also be able to communicate with other agent-hosting platforms, e.g. through the internet, in order to facilitate interaction between the different agents. Previous work by the authors has shown that the developed system can operate even through unreliable internet connections [21].

#### 5 Conclusions – Future Work

This paper presented the validation of an approach for control and optimisation of groups of energy hubs, which contain distributed energy resources interacting with multiple energy carriers. The structure of a hierarchical multi-agent system was described, which controls and coordinates the energy hubs, the energy hub elements, as well as two types of aggregators. The operational procedure of the multi-agent system has been described and its fundamental elements have been illustrated.

Different layers and functionalities of coordination were described. The overarching control structure was defined as a Virtual Power Plant, capable of interacting with external markets. Energy hubs are also grouped through a technical aggregation layer. Each individual energy hub is responsible for optimising energy carrier input according to associated loads. Implementation of agent-based control on multiple energy carriers, in combination with the energy hubs concept, adds the flexibility, resilience and extensibility of multi-agent systems to the inclusivity of energy hubs.

Simulated and experimental case studies were performed. The simulated case studies have proven that optimisation methods can be used to reduce the cost and/or emissions associated with energy hub operation. In addition, it was shown that energy hubs can participate in energy-related markets while adhering to technical constraints. The proposed system has been found to reduce the cost of energy supply from the energy hub components by **6.42%** and the emissions by **14.10%**. In addition, the cost of balancing a mismatch is reduced by more than 50%, bringing final energy cost reductions. Hence, if such a system is scaled up to creating localised energy communities with millions of consumers, it would bring significant cost reductions, to the level of tens of £ millions. The next step in this research is to evaluate these costs through extending the sensitivity analysis of Section 3.4 with a realistic market participation case study, as this was beyond the remit of this paper.

Finally, the experimental case study provided further evidence, in addition to the work done in [21], that the mechanism to realise this functionality can be implemented on generic, cost-effective equipment, such as a personal computer and/or an inexpensive controller. The next step would be to develop a purpose-built controller that can also host the agent.

#### 6 Acknowledgements

Part of the work presented in this paper was supported by the Interreg IVA Channel programme 2007-2013 and the European Regional Development Fund (ERDF), through the project “Ecotec 21”, with project no. 4160.

#### 7 References

- [1] T. S. Ustun, C. Ozansoy, A. Zayegh, (2011), “Recent developments in microgrids and example cases around the world—A review”, *Renewable and Sustainable Energy Reviews*, Vol. 15, No. 8, pp. 4030-4041
- [2] N.W.A. Lidula, A.D. Rajapakse, (2011), “Microgrids research: A review of experimental microgrids and test systems”, *Renewable and Sustainable Energy Reviews*, Vol. 15, No. 1, pp. 186-202
- [3] S. Papathanassiou, N. Hatzargyriou and K. Strunz, (2005), “A benchmark low voltage microgrid network”, *CIGRE Symposium*, Athens, 13-16 April 2005
- [4] M. Chaudry, N. Jenkins, M. Qadrdan, J. Wu, (2014), “Combined gas and electricity network expansion planning”, *Applied Energy*, Vol. 113, January 2014, pp. 1171-1187
- [5] M. Geidl, G. Koepfel, P. Favre-Perrod, B. Klockl, G. Andersson, K. Frohlich, (2007), “Energy hubs for the future”, *IEEE Power and Energy Magazine*, Vol. 5, No. 1, pp.24-30, Jan.-Feb. 2007
- [6] M.T. Rees, J. Wu, B. Awad, J. Ekanayake, N. Jenkins, (2011), “A total energy approach to integrated community infrastructure design”, 2011 IEEE Power and Energy Society General Meeting, 24-29 July 2011
- [7] X. Liu, J. Wu, N. Jenkins, A. Bagdanavicius, (2015), “Combined analysis of electricity and heat networks”, *Applied Energy* (in press), <http://dx.doi.org/10.1016/j.apenergy.2015.01.102>

- 1 [8] M. Chaudry, N. Jenkins, G. Strbac, (2008), "Multi-time period combined gas and electricity network  
2 optimization", *Electric Power Systems Research*, Vol. 78, No. 7, July 2008, pp. 1265-1279
- 3 [9] M.D. Galus, G. Andersson, (2008), "Demand Management of Grid Connected Plug-In Hybrid Electric Vehicles  
4 (PHEV)", *IEEE Energy 2030 Conference (ENERGY 2008)*, 17-18 Nov. 2008
- 5 [10] S. Skarvelis-Kazakos, P. Papadopoulos, I. Grau Unda, (2014) "Agent-based control of multiple energy carriers  
6 and energy hubs", *5th IEEE PES International Conference and Exhibition on Innovative Smart Grid  
7 Technologies (ISGT Europe 2014)*, Istanbul, 12-15 October 2014
- 8 [11] P. Favre-Perrod, M. Geidl, B. Klockl, G. Koepfel, (2005), "A vision of future energy networks", *2005 IEEE Power  
9 Engineering Society Inaugural Conference and Exposition in Africa*, 11-15 July 2005
- 10 [12] M. Geidl, G. Andersson, (2005), "A modeling and optimization approach for multiple energy carrier power  
11 flow", *2005 IEEE Russia Power Tech*, 27-30 June 2005
- 12 [13] K. Orehounig, R. Evins, V. Dorer, (2015), "Integration of decentralized energy systems in neighbourhoods using  
13 the energy hub approach", *Applied Energy*, Vol. 154, 15 September 2015, pp. 277-289
- 14 [14] M. Geidl, G. Andersson, (2007), "Optimal Power Flow of Multiple Energy Carriers", *IEEE Transactions on Power  
15 Systems*, Vol. 22, No.1, pp.145-155
- 16 [15] A.L. Dimeas and N.D. Hatziargyriou, (2005), "Operation of a Multiagent System for Microgrid Control" *IEEE  
17 Transactions on Power Systems*, Vol. 20, No. 3, pp.1447-1455
- 18 [16] S.D.J. McArthur, E.M. Davidson, V.M. Catterson, A.L. Dimeas, N.D. Hatziargyriou, F. Ponci and T. Funabashi,  
19 (2007), "Multi-Agent Systems for Power Engineering Applications—Part I: Concepts, Approaches, and  
20 Technical Challenges," *IEEE Transactions on Power Systems*, Vol. 22, No. 4, pp.1743-1752
- 21 [17] K.H. van Dam, M. Houwing, Z. Lukszo, I. Bouwmans, (2008), "Agent-based control of distributed electricity  
22 generation with micro combined heat and power—Cross-sectoral learning for process and infrastructure  
23 engineers", *Computers & Chemical Engineering*, Vol. 32, No. 1–2, January 2008, pp. 205-217
- 24 [18] I. Grau Unda, P. Papadopoulos, S. Skarvelis-Kazakos, L. M. Cipcigan, N. Jenkins, E. Zabala, (2014),  
25 "Management of Electric Vehicle battery charging in distribution networks with Multi-Agent Systems", *Electric  
26 Power Systems Research*, Vol. 110, pp. 172–179
- 27 [19] A. F. Raab, M. Ferdowsi, E. Karfopoulos, I. Grau Unda, S. Skarvelis-Kazakos, P. Papadopoulos, E. Abbasi, L.M.  
28 Cipcigan, N. Jenkins, N. Hatziargyriou, and K. Strunz, (2011), "Virtual Power Plant Control Concepts with  
29 Electric Vehicles", *16th International Conference on Intelligent System Applications to Power Systems (ISAP)*,  
30 25-28 Sept. 2011, Crete, Greece
- 31 [20] P. Papadopoulos, N. Jenkins, L.M. Cipcigan, I. Grau, E. Zabala, (2013), "Coordination of the Charging of Electric  
32 Vehicles Using a Multi-Agent System", *IEEE Transactions on Smart Grid*, Vol.4, No.4, pp.1802-1809
- 33 [21] S. Skarvelis-Kazakos, E. Rikos, E. Kolentini, L.M. Cipcigan, N. Jenkins, (2013), "Implementing agent-based  
34 emissions trading for controlling Virtual Power Plant emissions", *Electric Power Systems Research*, Vol. 102,  
35 pp. 1-7, September 2013
- 36 [22] G. Chicco, P. Mancarella, (2009), "Distributed multi-generation: A comprehensive view", *Renewable and  
37 Sustainable Energy Reviews*, Vol. 13, No. 3, April 2009, pp. 535-551
- 38 [23] P. Mancarella, (2014), "MES (multi-energy systems): An overview of concepts and evaluation models", *Energy*,  
39 Vol. 65, pp. 1-17, February 2014
- 40 [24] X.Q. Kong, R.Z. Wang, X.H. Huang, (2007), "Energy optimization model for a, CCHP system with available gas  
41 turbines", *Appl Therm Eng*, 25:377–91
- 42 [25] K. Hemmes, J.L. Zachariah-Wolff, M. Geidl, G. Andersson, (2007), "Towards multisource, multi-product energy  
43 systems", *Int J Hydrogen Energy*, 32:1332–8
- 44 [26] M. Burer, K. Tanaka, D. Favrat, K. Yamada, (2003), "Multi-criteria optimization of a district cogeneration plant  
45 integrating a solid oxide fuel cell-gas turbine combined cycle, heat pumps and chillers", *Energy*, 28(6):497–518
- 46 [27] H. Li, R. Nalim, P.A. Haldi, (2006), "Thermal-economic optimization of a distributed multi-generation energy  
47 system—a case study of Beijing", *Appl Therm Eng*, 26(7):709–19
- 48 [28] A. Parisio, C. Del Vecchio & A. Vaccaro, (2012), "A robust optimization approach to energy hub management",  
49 *International Journal of Electrical Power & Energy Systems*, 42(1), 98-104
- 50 [29] A.L. Dimeas and N.D. Hatziargyriou, (2007), "Agent based control of Virtual Power Plants," *International  
51 Conference on Intelligent Systems Applications to Power Systems (ISAP) 2007*, 5-8 November 2007
- 52 [30] W. Ketter, J. Collins, P.P. Reddy, C.M. Flath & M.D. Weerdt, (2011), "The power trading agent competition",  
53 *ERIM Report Series Reference No. ERS-2011-027-LIS*
- 54 [31] S. Skarvelis-Kazakos, P. Papadopoulos, I. Grau, A. Gerber, L.M. Cipcigan, N. Jenkins and L. Carradore, (2010),  
55 "Carbon Optimized Virtual Power Plant with Electric Vehicles", *45th Universities Power Engineering  
56 Conference (UPEC)*, Cardiff, 31 August – 3 September 2010
- 57 [32] D. Pudjianto, C. Ramsay and G. Strbac, (2007), "Virtual power plant and system integration of distributed

- energy resources”, IET Renewable Power Generation, Vol. 1, No. 1, pp. 10–16
- [33] I. Lopez-Rodriguez, M. Hernandez-Tejera, (2015), “Infrastructure based on supernodes and software agents for the implementation of energy markets in demand-response programs”, Applied Energy, Vol. 158, pp. 1-11
- [34] E. Kuznetsova, Y. Li, C. Ruiz, E. Zio, (2014), “An integrated framework of agent-based modelling and robust optimization for microgrid energy management”, Applied Energy, Vol. 129, pp. 70-88
- [35] M.D. Galus, G. Andersson, (2009), “Integration of Plug-In Hybrid Electric Vehicles into energy networks”, 2009 IEEE Bucharest PowerTech, June 28 2009-July 2 2009
- [36] T. Krause, G. Andersson, K. Fröhlich, & A. Vaccaro, (2011), “Multiple-energy carriers: modeling of production, delivery, and consumption”, Proceedings of the IEEE, 99(1), 15-27
- [37] M. Moeini-Aghaie, P. Dehghanian, M. Fotuhi-Firuzabad, A. Abbaspour, (2014), “Multiagent Genetic Algorithm: An Online Probabilistic View on Economic Dispatch of Energy Hubs Constrained by Wind Availability”, IEEE Transactions on Sustainable Energy, Vol. 5, No.2, pp.699-708, April 2014
- [38] M. Wooldridge, (2009), “An introduction to multiagent systems”, John Wiley & Sons
- [39] L. Vincent, J. Marvin, H. Lucas, (2015), “Quarterly Energy Prices: June 2015”, National Statistics – Department of Energy & Climate Change, <https://www.gov.uk/government/organisations/department-of-energy-climatechange/about/statistics> (last visited 01 September 2015)
- [40] S. Skarvelis-Kazakos, L.M. Cipcigan and N. Jenkins, (2009), “Micro-Generation For 2050: Emissions Performances Of Micro-Generation Sources During Operation”, Pollack Periodica, Vol.4, No.2, pp.89-99
- [41] DTI Centre for Distributed Generation and Sustainable Electrical Energy, United Kingdom Generic Distribution System (UKGDS), <http://www.sedg.ac.uk> (last visited 01 September 2015)
- [42] S. Abu-Sharkh, R.J. Arnold, J. Kohler, R. Li, T. Markvart, J.N. Ross, K. Steemers, P. Wilson and R. Yao, (2006) “Can microgrids make a major contribution to UK energy supply?”, Renewable and Sustainable Energy Reviews, Vol. 10, No. 2, pp. 78-127
- [43] P. Pavon Mariño, “JOM (Java Optimization Modeler)”, <http://www.net2plan.com/jom/index.php> (last visited 01 September 2015)
- [44] A. Marinescu, C. Harris, I. Dusparic, S. Clarke, V. Cahill, (2013), “Residential electrical demand forecasting in very small scale: An evaluation of forecasting methods”, 2013 2nd International Workshop on Software Engineering Challenges for the Smart Grid (SE4SG), pp.25-32, 18 May 2013
- [45] J. Llanos, D. Saez, R. Palma-Behnke, A. Nunez, G. Jimenez-Estevez, (2012), “Load profile generator and load forecasting for a renewable based microgrid using Self Organizing Maps and neural networks”, The 2012 International Joint Conference on Neural Networks (IJCNN), 10-15 June 2012
- [46] National Audit Office, (2014), “Electricity Balancing Services”, Briefing for the House of Commons Energy and Climate Change Select Committee, May 2014